Int. J. Heat Mass Transfer. Vol. 35, No. 2, pp. 343–350, 1992
Printed in Great Britain

0017–9310/92 $5.00 + 0.00
Pergamon Press plc

Investigation of macrolayer thickness in nucleate pool boiling at high heat flux

A. K. RAJVANSHI
Department of Mechanical Engineering, Malviya Regional Engineering College, Jaipur, India

and

J. S. SAINI and R. PRAKASH
Department of Mechanical and Industrial Engineering, University of Roorkee, Roorkee, India

(*Received* 7 *June* 1989 *and in final form* 26 *December* 1990)

Abstract—The nucleate boiling at high heat flux is characterized by the existence of a liquid layer known as the macrolayer between the heating surface and the vapour mass. An analytical expression to predict the value of initial macrolayer thickness based on Helmholtz instability has been derived in terms of the thermophysical properties of the liquid and heat flux. The initial macrolayer thickness for different liquids has also been experimentally determined by the electrical resistance probe method. The predicted values have been compared with those obtained by experiment and a reasonably good agreement has been found.

INTRODUCTION

IT IS well known that in nucleate boiling under the high heat flux condition, the vertical coalescence of bubbles takes place at active sites forming vapour columns. The lateral coalescence of these vapour columns results in the formation of a vapour mass that entraps a liquid layer, known as the macrolayer, between a vapour mass and the heating surface, as illustrated in Fig. 1. As the vapour mass grows, the liquid in the macrolayer is consumed and the thickness of the macrolayer decreases. The maximum thickness of the macrolayer at the time of initiation of vapour mass is termed the initial macrolayer thickness. As the vapour mass departs, the bulk liquid impinges on the heated surface, thus destroying the identity of the macrolayer. Due to the impinging action of the relatively cold bulk liquid, the vapour stems on the heated surface get disturbed and a new cycle of vapour mass formation–growth and departure is thus initiated. This phenomenon is found to occur in the heat flux range between $0.6q_c$ and q_c [1].

The governing phenomenon of nucleate boiling heat transfer at high heat flux is the evaporation of the macrolayer. The heat transfer from the heating surface to the vapour mass takes place through the macrolayer. Therefore, the thickness of the macrolayer on the heating surface is an important parameter in the boiling heat transfer. However, direct measurement of the initial macrolayer thickness is not possible because it varies spatially as well as with time, and is also extremely thin. Therefore, some investigators tried to determine the initial macrolayer thickness by indirect methods.

Gaertner [1] obtained photographs of water boiling on a horizontal copper surface at high heat flux and determined the initial macrolayer thickness from the photographs. He correlated his experimental data with the experimental data of Gaertner and Westwater [2] on diameter of vapour stems and established the following relationship independently of heat flux:

$$\delta_0 = 0.6D. \tag{1}$$

Iida and Kobayasi [3] measured the time averaged void fraction in saturated pool boiling of water at atmospheric pressure by the probe method. They determined the initial macrolayer thickness by a plot of spatial variation of void fraction against the height from the heating surface. They found that the initial macrolayer thickness decreases with increasing heat flux.

Bhat *et al.* [4] determined the initial macrolayer thickness for water at atmospheric pressure using a

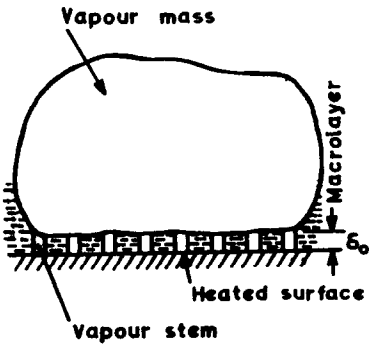

FIG. 1. Vapour mass formation near a heated surface in nucleate pool boiling at high heat flux.

NOMENCLATURE

A_v	cross-sectional area of vapour stems [m^2]
A_w	area of heated surface [m^2]
c_p	specific heat of liquid [J kg^{-1} K^{-1}]
D	diameter of vapour stem [m]
D_d	bubble departure diameter [m]
f	frequency of bubble/vapour mass emission [Hz]
h	height above the heating surface [m]
h_{fg}	latent heat of evaporation [J kg^{-1}]
N/A	active site density [m^{-2}]
q	heat flux [W m^{-2}]
q_c	critical heat flux [W m^{-2}]
ΔT	wall superheat [K]
t_d	bubble departure period [s]
t_l	time during which probe tip is in liquid [s]
u	average bubble rise velocity [m s^{-1}]
X	parameter.

Greek symbols

α	thermal diffusivity of liquid [m^2 s^{-1}]
δ_0	initial macrolayer thickness [m]
θ_0	average superheat [K]
λ_H	Helmholtz critical wavelength [m]
ρ_l	density of liquid [kg m^{-3}]
ρ_v	density of vapour [kg m^{-3}]
σ	surface tension [N m^{-1}].

plot of bubble and vapour mass frequency against the vertical distance from the heating surface. They measured the bubble and vapour mass frequencies above the heating surface by an electrical resistance probe.

Bhat *et al.* [5] hypothesized that the macrolayer is formed due to lateral coalescence of vapour stems on the top of the macrolayer and derived the following expression for initial macrolayer thickness:

$$\delta_0 = \frac{D}{2} + u(X^2 - t_d) \tag{2}$$

where

$$X = \frac{1}{2}\left[-\frac{1}{K_1} + \left(\frac{1}{K_1^2} + 4K_2\right)^{1/2}\right]$$

$$K_1 = \frac{u}{8M\theta_0}\left(\frac{fD_d}{u} - 1\right)$$

$$K_2 = \frac{1}{K_1}\left(\frac{D_0 - D_d}{4M\theta_0} + t_d^{1/2} + K_1 t_d\right)$$

$$M = \frac{\rho_l c_p \alpha^{1/2}}{\pi^{1/2}\rho_v h_{fg}}$$

$$\theta_0 = \frac{\Delta T}{2}$$

$$D_0 = \left(\frac{A}{N}\right)^{1/2}.$$

Experimental data on initial macrolayer thickness are not available in the literature for any liquid other than water. Data on diameter of vapour stems are required for predicting the initial macrolayer thickness from equations (1) and (2). In view of the fact that these data are also not available in the literature for any liquid except water, the present investigation was undertaken for generating experimental data on initial macrolayer thickness for various liquids. An analytical expression has also been derived for predicting the initial macrolayer thickness.

ANALYTICAL MODEL

Haramura and Katto [6] hypothesized that throughout the interference region, nucleate boiling is subject to Helmholtz instability, maintaining the boiling configuration of Fig. 1 up to the critical heat flux point. This view is quite different from the existing instability models where Helmholtz instability is assumed to be applicable at the critical heat flux point only. Besides, in the interference region, the vapour mass obstructs the feeding of liquid from the bulk region. Therefore, the way in which the heated surface is fed with liquid is governed by Helmholtz instability. Thus Helmholtz instability governs the phenomenon in the interference region in nucleate boiling, leading to the formation of a stable liquid film of a certain definite thickness on the heated surface.

Figure 2 illustrates tiny vapour jets anchored to active sites on a solid wall, corresponding to the observations made in experiments of saturated nucleate pool boiling at high heat fluxes. The liquid–vapour interface of the vapour jets is subjected to waves of various wavelengths; accordingly it must be unstable due to Helmholtz instability. However, the vapour jets are anchored to the solid wall, being nourished steadily with vapour, so that a liquid film including

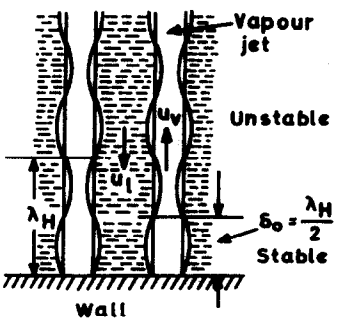

FIG. 2. Tiny vapour jets anchored to active sites on a solid wall at high heat flux.

vapour stems (causes of instability) can exist stably up to a distance δ_0 from the heated surface. The value of δ_0 depends on the unstable wavelength.

Haramura and Katto [6] hypothesized that the value of δ_0 lies between 0 and $\lambda_H/2$. The value of δ_0 decreases as the heat flux increases and is minimal at the critical heat flux, as indicated by the experimental results of many investigators [3, 4, 7–10]. Since δ_0 has much higher values in the interference region than at the critical heat flux, the highest value of δ_0 may be taken in the range specified by them. Therefore, δ_0 may be assumed to be equal to $\lambda_H/2$ [11], i.e.

$$\delta_0 = \frac{\lambda_H}{2}. \tag{3}$$

The critical wavelength for Helmholtz instability is given as [12]

$$\lambda_H = 2\pi\sigma\frac{\rho_l+\rho_v}{\rho_l\rho_v}\left(\frac{A_v}{A_w}\right)^2\left(\frac{\rho_v h_{fg}}{q}\right)^2. \tag{4}$$

Therefore, δ_0 may be expressed as

$$\delta_0 = \pi\sigma\frac{\rho_l+\rho_v}{\rho_l\rho_v}\left(\frac{A_v}{A_w}\right)^2\left(\frac{\rho_v h_{fg}}{q}\right)^2. \tag{5}$$

The experimental findings of Gaertner and Westwater [2] have shown that the magnitude of A_v/A_w is unaffected by heat flux. Haramura and Katto [6] derived the following relation for A_v/A_w:

$$\frac{A_v}{A_w} = 0.0584\left(\frac{\rho_v}{\rho_l}\right)^{0.2}. \tag{6}$$

Substituting the value of A_v/A_w from equation (6) into equation (5) gives

$$\delta_0 = 0.0107\sigma\rho_v\left(1+\frac{\rho_v}{\rho_l}\right)\left(\frac{\rho_v}{\rho_l}\right)^{0.4}\left(\frac{h_{fg}}{q}\right)^2. \tag{7}$$

For $\rho_v/\rho_l \ll 1$, equation (7) reduces to

$$\delta_0 = 0.0107\sigma\rho_v\left(\frac{\rho_v}{\rho_l}\right)^{0.4}\left(\frac{h_{fg}}{q}\right)^2. \tag{8}$$

EXPERIMENTAL APPARATUS

The apparatus shown in Fig. 3 was fabricated to obtain pool boiling data in the high heat flux region at atmospheric pressure using distilled water, methanol, ethanol, isopropanol, acetone and methyl ethyl ketone as the boiling liquids. Heat energy was generated electrically in a solid copper block (150 mm diameter, 200 mm long) by nine cartridge heaters each of 1 kW capacity inserted in the holes drilled in the block. The annular space between the heater rods and the copper block was filled with porcelain powder which conducted heat to the copper block and acted as a good electrical insulator. The power was supplied through a 10 KVA voltage stabilizer and adjustable autotransformer. A copper rod (50 mm diameter, 70 mm long) was used to conduct heat from the copper block to the boiling liquid. The copper conductor was fitted into a cavity on the top of the copper block after filling it with molten tin–lead solder alloy to provide good thermal contact between the mating surfaces. The heater assembly was placed in a mild steel box which was filled with glass wool insulation to reduce heat loss.

The copper conductor was taken inside the boiler vessel through a hole in the bottom plate. To ensure that boiling took place only on the top surface of the conductor, a teflon ring was fitted level with the top surface of the conductor and was supported on a stainless steel stand which was welded to the bottom plate. The teflon ring prevented the flow of heat from the copper conductor to other parts of the apparatus. Six 4 mm diameter holes were drilled in the conductor at 10 mm intervals each from the top surface to accommodate twin bored porcelain tubes containing chromel–constantan thermocouple wires. The thermocouple beads touched the central vertical axis of the conductor. The thermocouples were duly calibrated before being fixed in place. The heating surface was cleaned with a 4/0 grade emery paper. The surface roughness of the heating surface was measured by a light sectioning testing machine and was found to be equal to 9 μm.

The boiler vessel was made up of a stainless steel pipe of 135 mm internal diameter and 400 mm long. The vessel was fixed on a stainless steel plate with threads cut on the plate and vessel. Two 50 mm diameter plain glass windows were located near the bottom of the vessel to facilitate visual observation and photography of the boiling phenomenon. The outside surface of the boiler vessel was wrapped with a mica sheet and a nichrome wire in a glass wool sleeve was coiled over it to reduce heat loss and to keep the liquid at saturation temperature. The vapour formed during boiling was condensed in a single pass, parallel flow, tube and shell condenser. Before returning to the boiler vessel, the condensate was preheated to its saturation temperature by a nichrome wire coiled around the condensate pipe.

An electrical resistance probe was inserted into the vessel through a hole in the cover plate. The leakage through the hole was prevented by a pressure seal placed on the cover plate. The probe was held in a vertical position by a probe holder. The probe could be traversed in a vertical plane above the heating surface by means of a micrometer having a least count of 0.001 mm. The probe could be fixed in any position by tightening the screws on the probe holder. The heating surface was kept horizontal by levelling screws provided on the support for the heater and the mild steel box.

Details of the apparatus are given in ref. [7].

EXPERIMENTAL PROCEDURE

In each run, the heating surface was cleaned by a 4/0 grade emery paper. The boiler vessel was filled

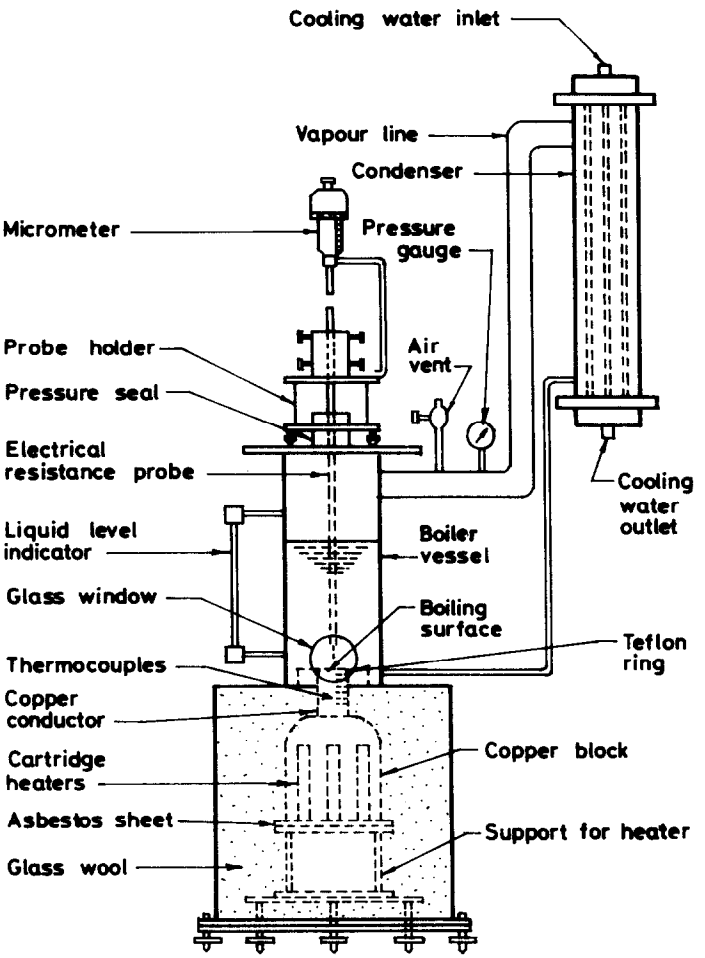

FIG. 3. Schematic diagram of the experimental set-up.

with about 3 l of test liquid and the main heater in the copper block and the auxiliary heaters on the boiler vessel and condensate return pipe were switched on. Energy input to the cartridge heaters was gradually increased to the required heat flux level. At low heat flux, increments of comparatively large magnitude could be given, whereas at high heat flux increments were limited to smaller values to avoid the sudden occurrence of film boiling. The liquid was allowed to boil for 2 h to remove dissolved gases in the liquid. After steady state was reached as indicated by the thermocouple readings, the experimental data were recorded. The heating surface temperature was determined by extrapolating the linear temperature profile which was obtained from the temperatures recorded by the thermocouples loated at various points along the axis of the copper conductor, whereas the heat flux was calculated by Fourier's equation for steady state, one-dimensional heat flow along the axis of the conductor. The saturation temperature of the boiling liquid was measured by a thermocouple suspended 40 mm above the heating surface. Many of the high heat flux runs were repeated several times to check the reproducibility of data and the agreement of data was found to lie within 10%.

Determination of initial macrolayer thickness

The initial macrolayer thickness was determined by an indirect method by plotting the bubble/vapour mass frequency as a function of height from the heating surface. The bubble/vapour mass frequencies were measured by feeding the output of the electrical resistance probe to a digital storage oscilloscope. The probe was traversed vertically downwards from a height of 3 mm above the heating surface and the bubble/vapour mass frequencies were measured at different points in a vertical plane. The principal of the probe method is based on utilizing the difference of electrical conductivity between the liquid and vapour. The detecting part consists of an insulated probe wire with an exposed tip projecting into the liquid and a plate electrode which is so large that the liquid is always in contact with it. The tip of the probe wire, with a diameter of 0.1 mm, was considered as the tiny elec-

trode while the heating surface, having a diameter of 50 mm, was considered to be the large plate electrode. The electrical resistance between these electrodes is determined by whether the tiny electrode is dipped in the liquid phase or in the vapour phase. Consequently, the voltage drop across the probe tip and heating surface gap is higher when the tip is in contact with vapour. The conductance of the medium within the gap between the probe tip and the heating surface decreases whenever a vapour mass or bubble strikes the tip of the probe wire and thus the output voltage signal decreases intermittently. The electrical circuit shown in Fig. 4 was devised for the measurement of bubble/vapour mass frequency. Direct current was supplied in the circuit by two 12 V batteries. The sweep on the oscilloscope screen was held at any instant and the number of voltage drops was counted. The bubble or vapour mass frequency was determined by dividing the number of voltage drops by the total sweep time at that instant. Each voltage drop of the oscilloscope beam represents a bubble/vapour mass emitted at that time and consequently the number of voltage drops observed on the oscilloscope screen over a fixed time interval can be interpreted as the bubble/vapour mass frequency. Since the bubble/vapour mass frequency is of random nature, five readings of the signal at each point were taken and averaged to obtain the bubble/vapour mass frequency at that point.

In each run during the experiment, electrical contact between the probe tip and the heating surface was made and then the probe was lifted to a height of 3 mm above the heating surface. The probe was traversed vertically downwards from this height by giving known micro-displacements to it by the vertical micrometer and the vapour mass frequency was measured at each location of the probe. The probe measures the vapour mass frequency except when it is very near (about 0.1 mm) the heating surface. The method of determination of initial macrolayer thickness is illustrated in Fig. 5. The vapour mass frequency is constant and is represented by the vertical line BC. When the probe is pushed to a point very close to the heating surface, it enters the macrolayer region. The frequency suddenly increases in this region because of bubbles emitted with very high frequency from the numerous active sites on the heating surface. Iida and Kobayasi [8] found that the average distance between the active sites is less than 1 mm in the high heat flux region. Therefore, when the probe is lowered further into the macrolayer region, it encounters the bubbles from the other active sites and the bubble emission frequency increases. The line DE in Fig. 5 represents the bubble frequency in the macrolayer region. The transition point at which the frequency suddenly changes from the vapour mass frequency to bubble frequency may be considered as the initial macrolayer thickness. This transition point, represented in Fig. 5 as A, is the point of intersection obtained by extrapolating the lines BC and ED.

The oscilloscope traces at vertical distances of 0.12 and 0.10 mm from the heating surface are shown in Figs. 6(a) and (b) respectively. The oscilloscope trace at a height of 0.12 mm, as seen in Fig. 6(a), shows voltage drops of higher order indicating that the probe tip remains in contact with vapour for longer periods. At this point, the probe tip remains in liquid for only 66.25 ms in a screen time of 204.75 ms. Hence the probe tip is in the vapour mass region. When the probe is lowered to a height of 0.10 mm, the frequency suddenly increases and voltage drops of smaller order

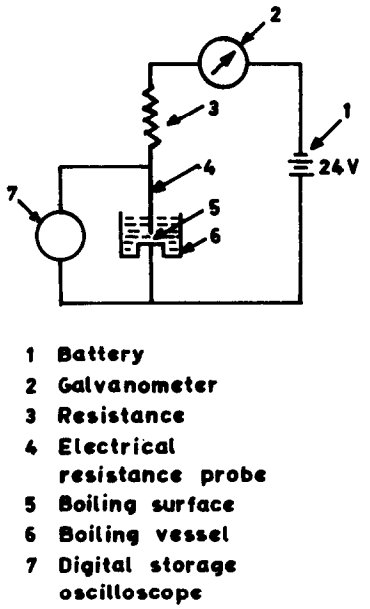

FIG. 4. Circuit diagram for bubble/vapour mass frequency measurement.

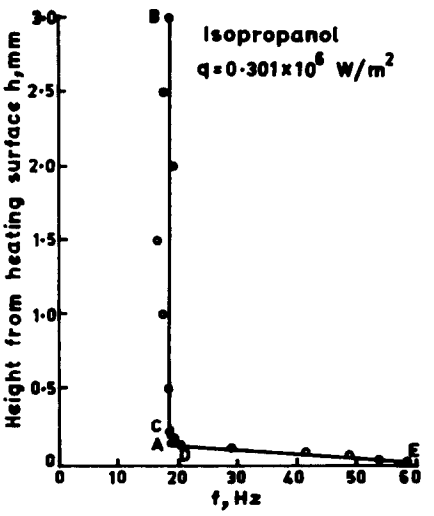

FIG. 5. Determination of initial macrolayer thickness from a frequency plot.

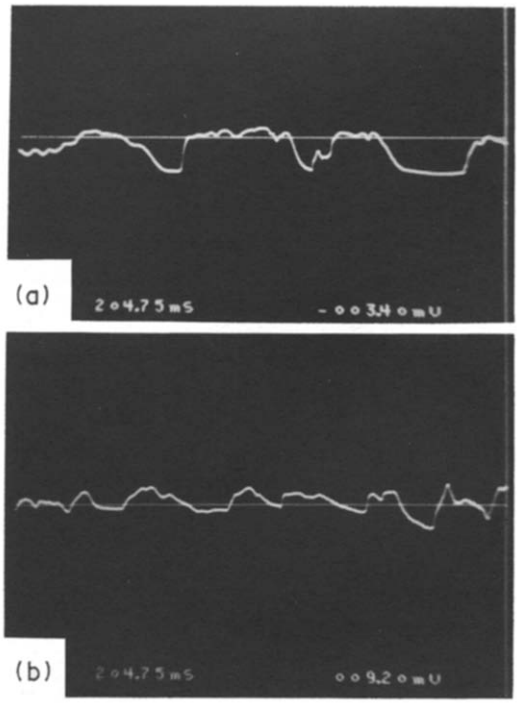

FIG. 6. Oscilloscope traces at different heights from the heating surface. (a) Vapour mass region: liquid, isopropanol; q, 0.301×10^6 W m^{-2}; h, 0.12 mm; f, 14.65 Hz; t_l, 66.25 ms. (b) Macrolayer region: liquid, isopropanol; q, 0.301×10^6 W m^{-2}; h, 0.10 mm; f, 29.30 Hz; t_l, 133.65 ms.

appear on the oscilloscope screen, as seen in Fig. 6(b), indicating that the probe tip remains in liquid for most of the time. At this point, the probe tip remains in liquid for 133.65 ms in a screen time of 204.75 ms. Hence it may be predicted that the probe tip has entered the macrolayer region where much smaller bubbles at high frequency are emitted from the active sites on the heating surface. Therefore, it may be concluded that the changeover from the vapour mass region to the macrolayer region takes place between these two points. The transition point A lies between these two points and can be determined by the extrapolation of the lines BC and ED. Therefore, the height of the point A above the heating surface can reasonably be interpreted as the initial macrolayer thickness [9]. The error in the determination of initial macrolayer thickness results from the extrapolation of the frequency plot, which is within ± 0.01 mm.

COMPARISON OF ANALYTICAL AND EXPERIMENTAL RESULTS

Figure 7 shows a comparison of the values of initial macrolayer thickness obtained from various expressions with the experimental data for water. It is seen that Gaertner's correlation predicts higher values, whereas Bhat *et al.*'s model [5] and the present model are in better agreement with the experimental data.

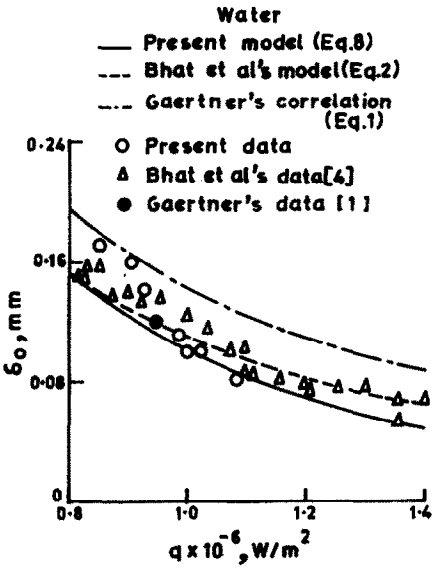

FIG. 7. Variation of initial macrolayer thickness with heat flux for water.

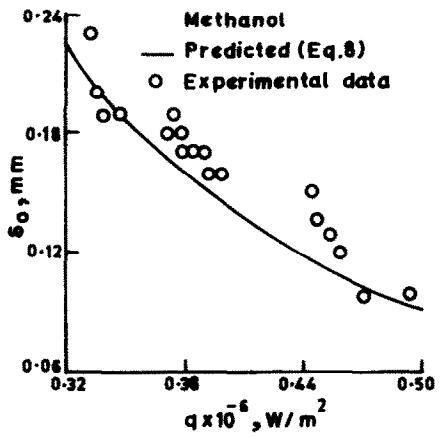

FIG. 8. Variation of initial macrolayer thickness with heat flux for methanol.

Equation (8) has also been compared with the experimental data for other liquids in Figs. 8–12. Since equations (1) and (2) require the experimental data on diameter of vapour stems for these liquids, which are not available in the literature, these expressions could not be compared with the experimental data for these liquids. The present model is found to be in fairly good agreement with experimental data for these liquids. A single point in the figures indicates a single measurement, except that of Gaertner's data point in Fig. 7 which is an average value.

Figure 13 is a composite plot which shows the deviation between the predicted and experimental values of initial macrolayer thickness for all the liquids. Most

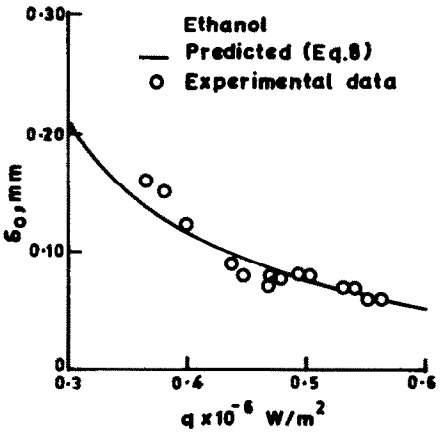

FIG. 9. Variation of initial macrolayer thickness with heat flux for ethanol.

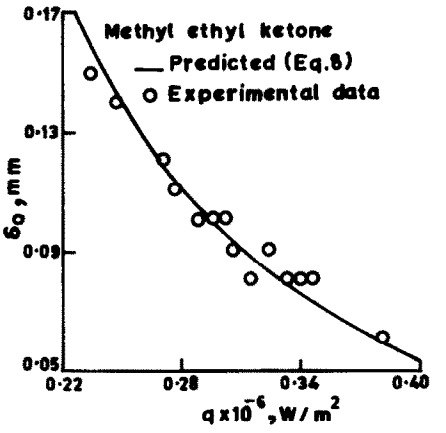

FIG. 12. Variation of initial macrolayer thickness with heat flux for methyl ethyl ketone.

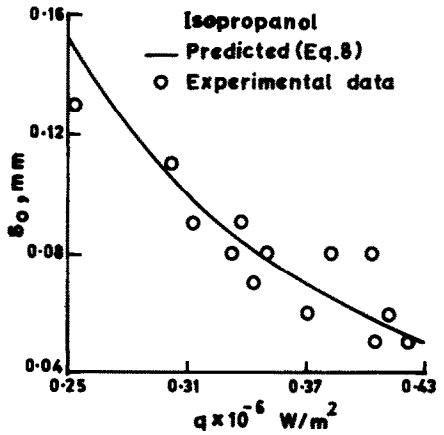

FIG. 10. Variation of initial macrolayer thickness with heat flux for isopropanol.

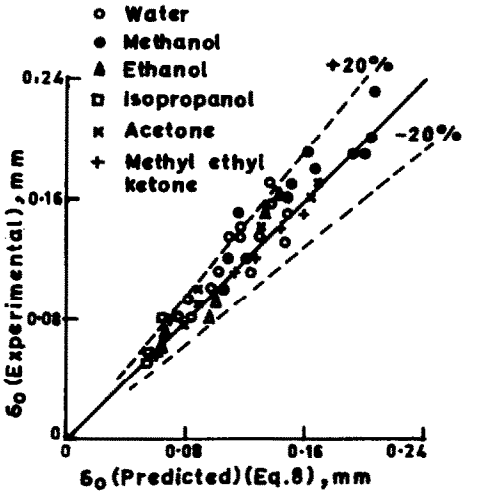

FIG. 13. Comparison between experimental and predicted values of initial macrolayer thickness.

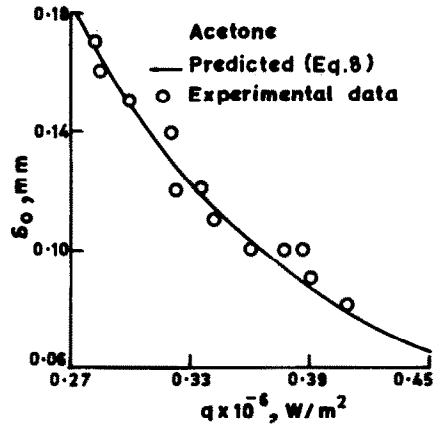

FIG. 11. Variation of initial macrolayer thickness with heat flux for acetone.

of the data points are seen to lie within the deviation limits of ±20%.

CONCLUSIONS

(1) The plot of frequency vs vertical distance from the heating surface can be successfully used to determine the initial macrolayer thickness in the high heat flux region of nucleate pool boiling.

(2) The expression derived on the basis of the proposed model of macrolayer formation based on Helmholtz instability is found to satisfactorily predict the value of initial macrolayer thickness with reasonable accuracy.

REFERENCES

1. R. F. Gaertner, Photographic study of nucleate pool boiling on a horizontal surface, *J. Heat Transfer* **87C**, 17–29 (1965).
2. R. F. Gaertner and J. W. Westwater, Population of

active sites in nucleate boiling heat transfer, *Chem. Engng Prog. Symp. Ser.* **56**(30), 39–48 (1960).
3. Y. Iida and K. Kobayasi, Distribution of void fraction above a horizontal heating surface in pool boiling, *Bull. JSME* **12**, 283–290 (1969).
4. A. M. Bhat, J. S. Saini and R. Prakash, Role of macrolayer evaporation in pool boiling at high heat flux, *Int. J. Heat Mass Transfer* **29**, 1953–1961 (1986).
5. A. M. Bhat, R. Prakash and J. S. Saini, On the mechanism of macrolayer formation in nucleate pool boiling at high heat flux, *Int. J. Heat Mass Transfer* **26**, 735–739 (1983).
6. Y. Haramura and Y. Katto, A new hydrodynamic model of critical heat flux, applicable widely to both pool and forced convection boiling on submerged bodies in saturated liquids, *Int. J. Heat Mass Transfer* **26**, 389–398 (1983).
7. A. K. Rajvanshi, Investigation of heat transfer phenomenon in nucleate pool boiling at high heat flux, Ph.D. Thesis, Department of Mechanical and Industrial Engineering, University of Roorkee, Roorkee, India (1989).
8. Y. Iida and K. Kobayasi, An experimental investigation on the mechanism of pool boiling phenomenon by a probe method, *Proc. Fourth Int. Heat Transfer Conf.*, Paper No. B 1.3 (1970).
9. A. K. Rajvanshi, J. S. Saini and R. Prakash, An experimental method for measurement of initial macrolayer thickness in nucleate pool boiling at high heat flux, *Proc. Tenth Natn. Heat and Mass Transfer Conf.*, Paper No. IV.9, Srinagar, India (1989). Reprinted in *Regional J. Heat Mass Transfer* **12**(2), 109–115 (1990).
10. Y. Katto and S. Yokoya, Principal mechanism of boiling crisis in pool boiling, *Int. J. Heat Mass Transfer* **11**, 993–1002 (1968).
11. A. K. Rajvanshi, J. S. Saini and R. Prakash, An analytical model of macrolayer formation in nucleate pool boiling at high heat flux, *Proc. Ninth Natn. Heat and Mass Transfer Conf.*, Paper No. HMT-33-87, Bangalore, India (1987). Reprinted in *Regional J. Heat Mass Transfer* **11**(3), 213–219 (1989).
12. S. Van Stralen and R. Cole, *Boiling Phenomena*, Vol. 2. Hemisphere, New York (1979).

ETUDE DE L'EPAISSEUR DE MACROCOUCHE DANS L'EBULLITION NUCLEEE EN RESERVOIR AVEC FLUX THERMIQUE ELEVE

Résumé—L'ébullition nucléée à flux thermique élevé est caractérisée par l'existence d'une couche liquide connue comme étant la macrocouche entre la surface chauffante et la masse de vapeur. Une expression analytique pour prédire la valeur de l'épaisseur initiale de cette macrocouche, basée sur l'instabilité de Helmholtz a été obtenue en fonction des propriétés thermophysiques du liquide et du flux thermique. L'épaisseur initiale pour différents liquides a été déterminée expérimentalement par la méthode de la sonde à résistance électrique. Les valeurs prédites sont comparées à celles obtenues par l'expérience et un accord raisonnable est trouvé.

UNTERSUCHUNG DER DICKE DER MAKROSCHICHT BEIM BLASENSIEDEN BEI HOHER WÄRMESTROMDICHTE

Zusammenfassung—Beim Blasensieden mit hoher Wärmestromdichte existiert zwischen der Heizfläche und dem Dampf eine Flüssigkeitsschicht, die Makroschicht genannt wird. Auf der Basis der Helmholz-Instabilität wird mit den thermophysikalischen Eigenschaften der Flüssigkeit und der Wärmestromdichte ein Ansatz abgeleitet, der die anfängliche Dicke der Makroschicht beschreibt. Für verschiedene Flüssigkeiten wurde die anfängliche Dicke der Makroschicht experimentell mit der elektrischen Widerstandssonde bestimmt. Die vorausberechneten Werte werden mit gemessenen verglichen, wobei sich eine recht gute Übereinstimmung ergibt.

ОПРЕДЕЛЕНИЕ ТОЛЩИНЫ МАКРОСЛОЯ В ПРОЦЕССЕ ПУЗЫРЬКОВОГО КИПЕНИЯ В БОЛЬШОМ ОБЪЕМЕ ПРИ ВЫСОКОЙ ПЛОТНОСТИ ТЕПЛОВОГО ПОТОКА

Аннотация—Пузырьковое кипение при высокой плотности теплового потока характеризуется наличием слоя жидкости, представляющего собой макрослой между поверхностью нагрева и объемом пара. Выведено аналитическое выражение для расчета величины начальной толщины макрослоя на основе неустойчивости Гельмгольца, учитывающее теплофизические свойства жидкости и плотность теплового потока. Начальная толщина макрослоя для различных жидкостей определялась также экспериментально. С использованием датчика электрического сопротивления получено хорошее согласие между теоретическими результатами и экспериментальными данными.